

ASCA observations of deep ROSAT fields V. The X-ray spectrum of hard X-ray selected QSOs.

A. Pappa^{1,*}, G.C. Stewart¹, I. Georgantopoulos², R.E. Griffiths³, B.J. Boyle⁴ and T. Shanks⁵

Department of Physics and Astronomy, University of Leicester, Leicester, LE1 7RH
National Observatory of Athens, Lofos Koufou, Palaia Penteli, 15236, Athens, Greece
Physics Department, Carnegie Mellon University, Pittsburgh, PA
Physics department, University of Durham, Science Labs, South Road, DH1 3LE
Anglo-Australian Observatory, Epping, Australia

29 October 2018

ABSTRACT

We present an analysis of the *ROSAT* and *ASCA* spectra of 21 broad line AGN (QSOs) with $z \sim 1$ detected in the 2–10 keV band with the *ASCA GIS*. The summed spectrum in the *ASCA* band is well described by a power-law with $\Gamma = 1.56 \pm 0.18$, flatter than the average spectral index of bright QSOs and consistent with the spectrum of the X-ray background in this band. The flat spectrum in the *ASCA* band could be explained by only a moderate absorption ($\sim 10^{22} \text{cm}^{-2}$) assuming the typical AGN spectrum is a power-law with $\Gamma=1.9$. This could in principle suggest that some of the highly obscured AGN, required by most X-ray background synthesis models, may be associated with normal blue QSOs rather than narrow-line AGN. However, the combined 0.5–8 keV *ASCA-ROSAT* spectrum is well fit by a power-law of $\Gamma = 1.7 \pm 0.2$ with a spectral upturn at soft energies. It has been pointed out that such an upturn may be an artefact of uncertainties in the calibration of the *ROSAT* or *ASCA* detectors. Nevertheless if real, it could imply that the above absorption model suggested by the *ASCA* data alone is ruled out. Then a large fraction of QSOs could have “concave” spectra i.e. they gradually steepen towards softer energies. This result is in agreement with the *BeppoSAX* hardness ratio analysis of ~ 100 hard X-ray selected sources.

Key words: surveys – galaxies: active – quasars:general – X-rays:general

1 INTRODUCTION

It has been almost 40 years since Giacconi et al. (1962) discovered the X-ray Background (XRB), the first cosmic background detected. Nevertheless its origin is still not fully understood. At a flux limit of $\sim 10^{-15} \text{erg cm}^{-2} \text{s}^{-1}$ 70–80% of the soft 0.5–2 keV XRB is resolved into discrete sources and the majority of these are QSOs i.e. broad line AGN (Schmidt et al. 1998). However, the spectrum of nearby, bright AGN is inconsistent with the spectrum of the X-ray background. This is known as the “spectral paradox” (Boldt 1987). Indeed, *HEAO-1*, *ASCA* and *BeppoSAX* observations have shown that the XRB spectrum in the 1–10 keV band has a spectral index of $\Gamma = 1.4$ (Marshall et al. 1980, Gendreau et al. 1995, Miyaji et al. 1998, Vecchi et al. 1999). On the other hand the nearby radio-quiet QSOs typically have a significantly softer spectrum, with $\Gamma \sim 1.8$, (Lawson et al.

1997, Reeves et al. 1997) and therefore they can contribute only a small fraction of the XRB.

In the hard X-ray band (2–10 keV) only $\sim 30\%$ of the XRB has been resolved into discrete sources (with *ASCA* and *BeppoSAX*) down to a flux limit of $\sim 5 \times 10^{-14} \text{erg cm}^{-2} \text{s}^{-1}$ (Georgantopoulos et al. 1997, Cagnoni et al. 1998, Giommi et al. 2000, Akiyama et al. 2000). The number-count distribution, $\log N$ - $\log S$ in the 2–10 keV band, is about a factor of two above the *ROSAT* counts, assuming a photon spectral index of $\Gamma = 2$ for the *ROSAT* sources. This suggests the presence of a population with flat or absorbed spectra. Setti & Woltjer (1979) first suggested that the entire extragalactic X-ray light could be explained in the context of a simple unified scheme for AGNs. Several models have been developed along these lines (e.g. Comastri et al. 1995) which provide good fits to the XRB and the X-ray source counts. All these assume that the XRB consists of a mix of AGNs obscured by a range of column densities. However, only a small number of obscured high redshift AGN have been detected so far in *ASCA* and *BeppoSAX* surveys

* Present address: Institute for Astronomy, University of Edinburgh, Royal Observatory, Blackford Hill, Edinburgh EH9 3HJ.

(eg Ohta et al. 1996, Boyle et al. 1998a, Georgantopoulos et al. 1999, Fiore et al. 1999).

The deep *Chandra* surveys deepened the riddle of the origin of the XRB even further. In the hard 2-10 keV band they probed fluxes at least an order of magnitude deeper than *ASCA* (Mushotzky et al. 2000) albeit with limited number statistics due to the small field-of-view of ACIS on-board *Chandra*. A large fraction of the detected sources is associated with QSOs which appear to have steep spectra. Surprisingly, no numerous, clearcut examples of the putative obscured AGN population at high redshift have yet been found. Instead, two 'new' populations emerged which are associated with either early-type galaxies or extremely faint optical counterparts.

Here, we derive the broad-band (0.5-8 keV) spectral properties of the 'typical' (ie high redshift, faint) hard X-ray selected QSOs in our *ASCA* survey. These contribute a large fraction of the XRB and therefore comparison of their spectrum with that of the XRB is expected to shed more light on the spectral paradox. We note that our objects span a wide range of redshifts, and hence no physical significance should be attributed to the models applied and no straightforward constraints on the AGN accretion physics can be derived. In contrast the aim of our analysis is to parameterise the "average" QSO spectrum over a large redshift range and compare it with that of the cosmic XRB.

2 THE SAMPLE

We have performed an *ASCA* follow-up (Georgantopoulos et al. 1997) of our deep *ROSAT* survey (Georgantopoulos et al. 1996). We have observed 6 fields (SGP2, QSF1, QSF3, GSGP4, BJS855, BJS864) and in our first, quick-look analysis, we detected 39 sources down to a flux limit of $S_{(2-10\text{keV})} \sim 5 \times 10^{-14} \text{erg cm}^{-2} \text{s}^{-1}$ in the 2-10 keV band. We obtained optical identifications for the vast majority of our sources using the 3.9m AAT telescope. Most (21 objects) are QSOs. All but one (AXJ1343.5-0004) have been detected in the soft X-rays by *ROSAT*. AXJ1343.5-0004 is identified as a UV excess quasar from Boyle et al. 1990. Their redshifts range from $z=0.145$ to $z=1.952$ with a mean of $z \sim 1$ (see Georgantopoulos et al. 1997 and Boyle et al. 1998b) There is also evidence for the presence of QSOs obscured in X-rays with some modest amount of reddening. These objects have narrow lines in the optical range but they clearly present broad lines in their infrared spectra (eg Georgantopoulos et al. 1999).

Only a small fraction of our sources are radio-loud. We cross correlated the list of our QSOs with the NRAO VLA Sky Survey (NVSS) list of radio sources (Condon et al. 1998). The NVSS covers the sky north of J2000 $\delta = -40^\circ$ at 1.4 GHz down to a flux limit of $S=2.5$ mJy. Therefore it does not cover our QSF1 and QSF3 fields. Of 12 QSOs in the other three fields, one has a possible NVSS counterpart within 1 arcmin. The probability of finding a source within 1 arcmin of an arbitrary position is 0.0145. Boyle et al. (1993, 1995) made a deep observation at 1.472 GHz with the Australia Telescope Compact Array of the QSF3 field. They found 6 coincidences within 15 arcsec. Out of our 6 QSOs in the field only one (AX J0342.0-4403) is associated

with a radio source. Hereafter, we include the two (possible) radio-loud QSOs in our analysis.

3 DATA REDUCTION AND ANALYSIS

We observed 6 fields from our *ROSAT* survey with *ASCA* (Tanaka, Inoue & Holt 1994). Here we present the analysis of the GIS data alone, because (a) the GIS field of view matches that used in our *ROSAT* survey and (b) with the GIS we maximize the effective exposure times after rejecting time periods with high rates of particle events. In table 1. we give the field names in column (1), equatorial coordinates (J2000) in columns (2) and (3), the Galactic hydrogen column density in units of 10^{20}cm^{-2} (Stark et al. 1992) in column (4), the number of QSOs detected in each field (5), the net *ASCA* exposure times per field in ks in column (6) and the net *ROSAT* exposure times in ks in column (7). The QSF3 field was observed with *ASCA* in 1993 June and 1993 September during the period of performance verification phase (PV phase). The GSGP4, BJS855, QSF1, SGP2 and BJS864 fields were observed in 1994 June, 1995 November, 1997 January, 1997 July and January 1998 respectively. Details of the *ROSAT* observations are given in Blair et al. 2000. In table 2 we present the list of QSOs. The names are given in column (1), their *ASCA* position in column (2), the redshift of their optical counterpart (3), the count rate in the 1-2 keV and 2-10 keV bands in (4) and (5) respectively and their 2-10 keV flux in column (6); in column (7) the hardness ratio; in column (8) the radio flux (mJy) is given. The X-ray fluxes are estimated for a single power-law model with $\Gamma=1.56$ and Galactic absorption. This model was chosen because it describes the *ASCA* data adequately (see §4.2). If, on the other hand, we use the standard AGN spectrum, namely a single power-law with $\Gamma=1.7$, the obtained fluxes are $\sim 5\%$ lower.

We used the standard 'Revision 2' (see the *ASCA* Data Reduction Guide) processed data from the Goddard Space Flight Center (GSFC). As our sources are quite faint, we used a circular source region centered on the source of only 1 arcmin radius, which includes 33 per cent of the total energy. In addition, by using such a small region we avoid overlapping of extraction regions, since some of our sources lie close to each other. Background counts were estimated from a source-free circular region centered in the field of view of the GIS detector. Because our sources lie at different off-axis angles we took into account the vignetting, by correcting the source counts for this effect. We also corrected the counts taking into account the light falling out of the 1 arcmin extraction radius. The spectral fitting was performed with XSPEC v10. The spectra were rebinned such that each resultant channel had at least 20 counts per bin (source+background), which permitted us to use χ^2 minimizations for spectral fitting. Due to considerable contamination from the Galactic background as well as some uncertainties in the low energy calibration of *ASCA* (George et al. 1998) we restricted our spectral analysis to the 0.8-8.0 keV energy band. Above 8 keV the signal-to-noise drops rapidly and thus we choose to ignore these data.

Table 1. List of ASCA fields

Field	R.A.	Dec.	N_H	number	ASCA exposure	ROSAT exposure
(1)	J2000	J2000	($\times 10^{20} \text{cm}^{-2}$)	of QSOS	(ksec)	(ksec)
(1)	(2)	(3)	(4)	(5)	(6)	(7)
QSF3	03 41 44.4	-44 07 04.8	1.7	6	78	52
QSF1	03 42 10.4	-44 54 38.5	1.7	3	44	49
SGP2	00 52 08.7	-29 05 00.6	1.8	3	50	24
GSGP4	00 57 29.78	-27 37 21.0	1.8	4	41	47
BJS855	10 46 21.36	-00 20 17.8	1.8	2	46	27
BJS864	10 46 21.36	-00 20 17.8	1.9	3	45	23

Table 2. The list of the QSOs in the 6 fields. The columns contain the following information: (1) The source name; (2) ASCA position of the object; (3) The redshift of the optical counterpart; (4) ASCA GIS count rate in the 1-2 keV band, together with the photon errors in units of $10^{-3} \text{ count s}^{-1}$; (5) same as (4) but in 2-10 keV band; (6) ASCA GIS flux in the 2-10 keV band for a power-law with $\Gamma=1.56$ and Galactic absorption in units of $\times 10^{-14} \text{ erg s}^{-1} \text{ cm}^{-2}$; (7) hardness ratio; (8) flux at 1.4 GHz in *mJy*.

Name	ASCA position	z	count rate	count rate	ASCA flux	HR	$S_{1.4\text{GHz}}$
(1)	(2)	(3)	1-2 keV	2-10 keV	2-10 keV	(7)	(8)
(1)	(2)	(3)	(4)	(5)	(6)	(7)	(8)
AX J0050.8-2902	00 50 53.8 -29 02 16	0.428	2.1 ± 0.2	2.7 ± 0.3	16.5 ± 1.7	$+0.1 \pm 0.1$	< 2.5
AX J0051.9-2913	00 51 56.7 -29 13 56	2.056	0.6 ± 1.3	1.4 ± 0.2	8.2 ± 1.1	$+0.3 \pm 0.3$	< 2.5
AX J0053.0-2927	00 53 05.1 -29 11 39	0.830	1.3 ± 0.2	2.1 ± 0.3	13.0 ± 1.6	$+0.3 \pm 0.1$	< 2.5
AX J0056.4-2748	00 56 25.6 -27 48 48	0.145	9.1 ± 0.7	6.1 ± 0.5	30.7 ± 2.8	-0.2 ± 0.1	< 2.5
AX J0056.5-2729	00 56 31.1 -27 29 47	1.010	3.0 ± 0.5	2.5 ± 0.3	15.2 ± 1.8	-0.1 ± 0.1	0.086
AX J0057.3-2731	00 57 20.8 -27 31 53	1.209	2.8 ± 0.5	1.9 ± 0.3	11.7 ± 1.6	-0.2 ± 0.1	< 2.5
AX J0057.8-2735	00 57 48.4 -27 35 56	0.57	< 0.2	0.8 ± 0.3	3.70 ± 1.7	> 0.5	< 2.5
AX J0342.4-4511	03 42 27.0 -45 11 58	0.443	1.7 ± 0.3	3.0 ± 0.3	18.1 ± 1.8	$+0.3 \pm 0.2$	-
AX J0343.2-4451	03 43 16.3 -44 51 44	1.410	1.3 ± 0.3	2.2 ± 0.2	13.3 ± 1.5	$+0.3 \pm 0.1$	-
AX J0342.5-4502	03 42 35.0 -45 02 19	0.185	1.1 ± 0.3	1.6 ± 0.2	9.5 ± 1.2	$+0.2 \pm 0.1$	-
AX J0341.1-4412	03 41 04.5 -44 12 04	1.808	0.8 ± 0.1	1.2 ± 0.4	7.2 ± 2.2	$+0.2 \pm 0.2$	$< 0.125^*$
AX J0341.4-4410	03 41 23.0 -44 10 47	0.505	< 0.2	1.0 ± 0.3	6.1 ± 1.7	> 0.6	$< 0.125^*$
AX J0342.0-4410	03 42 01.1 -44 10 53	1.840	< 0.1	1.3 ± 0.3	7.6 ± 1.7	> 0.8	$< 0.125^*$
AX J0342.0-4403	03 42 02.4 -44 03 51	0.635	< 0.1	1.0 ± 0.3	6.0 ± 1.8	> 0.7	0.142*
AX J0342.3-4412	03 42 19.1 -44 12 38	1.091	< 0.3	0.8 ± 0.3	4.9 ± 1.9	> 0.2	$< 0.125^*$
AX J0342.6-4404	03 42 35.4 -44 04 41	0.377	0.2 ± 0.3	1.4 ± 0.4	8.4 ± 2.5	$+0.7 \pm 0.3$	$< 0.125^*$
AX J1046.1-0020	10 46 05.1 -00 20 48	1.070	0.5 ± 0.1	0.9 ± 0.1	5.4 ± 0.6	$+0.3 \pm 0.1$	< 2.5
AX J1046.2-0022	10 46 13.4 -00 22 16	1.952	< 0.4	1.9 ± 0.1	5.3 ± 0.6	> 0.6	< 2.5
AX J1344.6-0015	13 44 57.8 -00 15 09	0.244	6.4 ± 0.5	5.9 ± 0.5	35.6 ± 2.8	-0.1 ± 0.1	< 2.5
AX J1343.5-0004*	13 43 26.0 -00 16 14	1.511	< 0.2	1.2 ± 0.2	7.0 ± 1.1	> 0.6	< 2.5
AX J1343.3-0016	13 43 51.8 -00 04 41	1.14	< 0.3	2.4 ± 0.3	14.4 ± 1.7	> 0.7	< 2.5

* From Boyle et al. 1995.

* object not detected with ROSAT.

4 X-RAY SPECTRUM

4.1 Individual source spectra

Since the photons from the individual QSOs are too few to give reliable spectra, clues for the properties of each QSO come from their hardness ratios (HR). Here we define the hardness ratio as $h-s/h+s$, where h and s are the total number of counts, in the 2-10 keV and 1-2 keV bands respectively. In the case where there was no detection in the 1-2 keV band, we estimate the 3σ upper limit following Kraft et al. (1991). We test for possible systematic biases that may arise due to the combined energy and radial dependence of the PSF, by splitting the entire sample into sources lying within the 12-arcmin radius from the center of the GIS and those lying beyond. Additionally, we created simulated spectra of sources lying at various distances from the center and estimated their hardness ratio. No trend in HR with off-axis angle is apparent at any flux and spectral shape. In

fig. 1 the hardness ratio of each object versus the observed flux in the 2-10 keV band is shown. The hardness ratios for four different power-law models assuming Galactic absorption are shown (left hand scale). The right hand scale indicates the expected spectrum in the case of $\Gamma = 1.9$ for different absorbing column densities. One interesting result is that although our objects are optically classified as QSOs, the data require a moderate absorption ($\sim 10^{22} \text{cm}^{-2}$) in order to reproduce the flat spectra observed. The number of sources with flat spectra increases towards faint fluxes, (and hence the mean spectrum flattens) suggesting the emergence of a hard X-ray QSO population. This is in agreement with previous results by Ueda et al. (1999) as well as results from hard X-ray selected type I AGN with *BeppoSAX* and *Chandra* (Della Ceca et al. (1999); Fiore et al. 2001). In addition our result is in agreement with the hardness ratio analysis of ~ 100 hard X-ray selected sources by Giommi et al. 2000.

Before interpreting this result we examined whether

the observed flattening is due to systematic effects. As our sources are faint a possible source of systematic errors is the background subtraction. Since the spectrum of the X-ray background is flat ($\Gamma \sim 1.4$), any over-subtraction of the background will produce a flat spectrum. This effect will be apparent at faint sources close to the limit of the survey, since at this faint limit, the sources have fluxes comparable to that of the background. At higher fluxes this effect will be negligible. Another source of systematic effects, suggested by Della Ceca et al. 1999, may be due to spectral bias in the source selection. They showed that for sources with same flux but different spectra, different number of counts will be detected. As we approach the flux limit of the survey, sources with a favourable spectrum will be detected, whereas sources with the same flux but with an unfavourable spectrum will be missed. However they showed that in the case of the *ASCA* GIS, this selection effect favours the detection of steep spectrum sources. In addition to this, it is clear from Fig. 1 that the hardening of the spectra is observed in the brighter data as well. The last two arguments give support to the reality of the observed trend.

The flattening could be attributed to intrinsic absorption. Indeed, a relatively small amount of absorption ($< 10^{22} \text{ cm}^{-2}$) could easily yield an effective index of $\Gamma \sim 1.5$. Some high redshift QSOs with high column densities have been found in the HELLAS 5-10 keV *BeppoSAX* survey (Fiore et al. 2000) and elsewhere (Georgantopoulos et al. 1999, Boyle et al. 1998, Halpern et al. 1998, Akiyama et al. 2000, Reeves & Turner 2000). Recently, Norman et al. 2001, detected a further example of a type II QSO in the *Chandra* Deep Field South; CDF-S 202. However the *Chandra* surveys have failed to detect a large number of clear-cut examples of this population of object as yet. As we have redshifts for our sample we can explore further the origin of this spectral flattening. For example, Vikhlinin et al. (1995) suggested that absorbed QSO spectra may originate due to damped *Ly α* clouds associated with protogalaxies. We plot the hardness ratio versus the redshift in Fig. 2. There is no clear trend for spectral evolution with redshift. We then examined whether the flattening of the spectrum is due to spectral evolution with luminosity. We plot the hardness ratio versus the 2-10 keV luminosity in Fig. 3. Again no trend for spectral evolution with luminosity is apparent.

4.2 The integrated QSO spectrum

Here we derive the average X-ray spectrum stacking together the QSOs photons in each field. Firstly we fit the *ASCA* data alone in the 0.8-8.0 keV energy band, forcing the two GIS detectors to have the same normalisations and we tie the spectral index for the power-law component to take the same value in all data sets. We find that a single power law (PL) with $\Gamma = 1.56 \pm 0.18$ for $\chi^2 = 104.89/99$ degrees of freedom (d.o.f.) with the hydrogen column density fixed to the Galactic value (in the range of $1.7 \times 10^{20} \text{ cm}^{-2} - 1.9 \times 10^{20} \text{ cm}^{-2}$) is a reasonable fit, in perfect with the hardness ratio analysis.

We then fit the *ROSAT* data. Again, we tie the spectral index for the power-law component to take the same value in all data sets, over the 0.5-2.0 keV range. We fit the data with a single power-law component and we obtain a slope of $\Gamma = 2.32 \pm 0.2$ ($\chi^2 = 170.23/173$ d.o.f.). Over the full 0.1-2.0

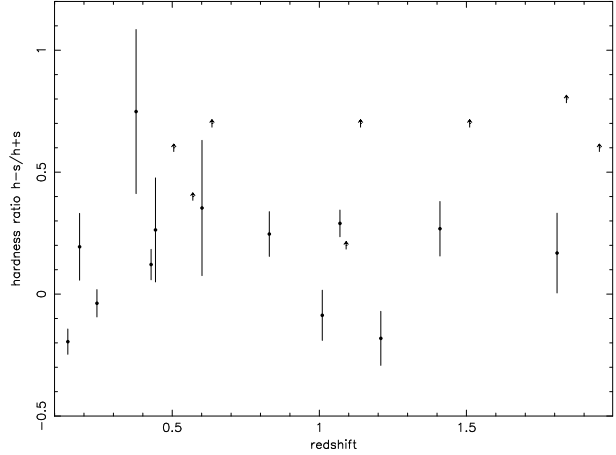


Figure 2. The HR versus the redshift of the sources.

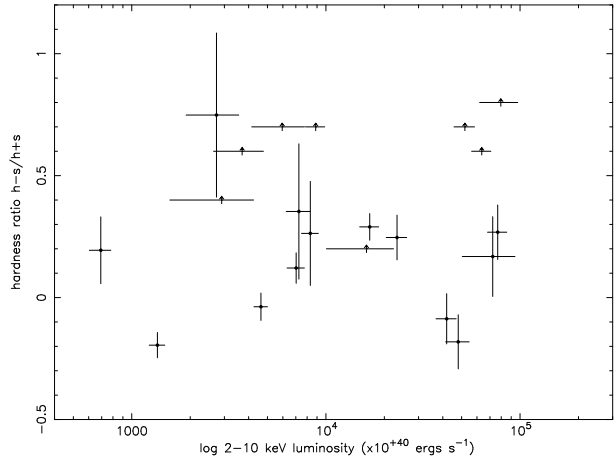


Figure 3. The HR versus the 2-10 keV luminosity.

keV range a single power-law gives a poor fit ($\Gamma = 2.44$ with $\chi^2 = 690/333$ d.o.f.).

A joint *ASCA* -*ROSAT* fit over the 0.5-8.0 keV energy range was carried out as well. The single power-law fit gives $\Gamma = 2.16 \pm 0.1$ ($N_H = \text{Galactic}$ and $\chi^2 = 309.21/273$ d.o.f.). However, the obtained spectral index is clearly discrepant with the *ASCA* data alone, while it is in good agreement with the *ROSAT* data. This is attributed to the better statistics of the *ROSAT* data compared to *ASCA*, which drive the spectral fitting, while it has been suggested that the spectral index discrepancy may be due to calibration uncertainties in the PSPC and GIS response matrices causing a fake soft excess (Iwasawa, Nandra, Fabian 1999). We have parameterised this spectral upturn with a broken power-law model (BKN PL model). In this case the soft and hard components of the spectrum are represented by two power-law with spectral indices Γ_1 and Γ_2 , respectively. We obtained a good fit with $\Gamma_1 = 2.35^{+0.11}_{-0.11}$ and $\Gamma_2 = 1.47^{+0.22}_{-0.20}$ and a break point for the energy of $1.48^{+0.32}_{-0.19}$ keV. It is clear that these are in agreement with the indices obtained by fitting the data of each detector alone.

We then added a soft-excess black-body component with $kT=0.1$ keV to the joint *ROSAT* -*ASCA* fit (PL+BB model). In this case we obtain a good fit as well ($\chi^2 = 271.46/261$ d.o.f.), with $\Gamma = 1.71^{+0.19}_{-0.17}$. The value of the slope

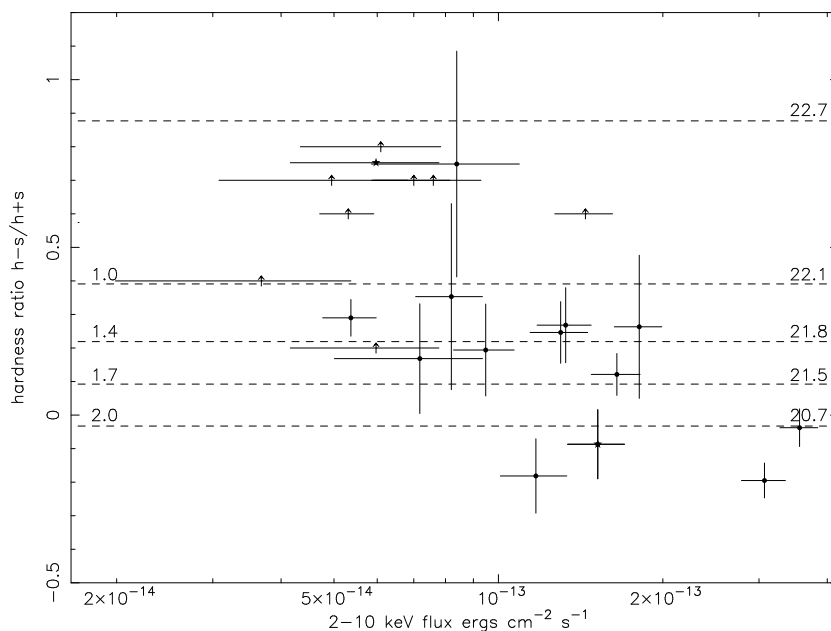


Figure 1. The hardness ratio (HR) versus flux for our QSOs with predicted HRs for various power-law indices (left hand scale) and for a power-law with $\Gamma = 1.9$ and a range of absorption (right hand scale). The two with possible radio counterparts are shown (stars). Arrows indicate lower limits.

is consistent within the 90 percent errors bars, with the slope obtained by fitting the *ASCA* data alone. The parameters derived when including the blackbody component are in excellent agreement with the findings of Blair et al. (2000). The above authors derived the average ROSAT spectrum of soft X-ray selected QSOs using 150 objects. They splitted the sample in five redshift bins and they obtained a power-law slope of $\Gamma = 1.8 - 1.9$ (and a soft excess with $kT=0.1$ keV), in all bins. We emphasize that although the above models parameterise successfully the data, no real physical significance should be attributed. This is due to the fact that our data span a wide range of redshifts and therefore the resulting spectrum is a blend of various spectral features at different rest-frame energies. However, the requirement of the data for this component clearly demonstrates the need for a spectral upturn at low energies (below ~ 2 keV). A summary of the fits is shown in Table 3.

5 DISCUSSION AND CONCLUSIONS

We investigate the properties of the typical, high redshift, hard X-ray selected QSOs using a sample of 21 objects detected in six deep *ASCA* fields. The hardness ratio analysis showed that the source spectra harden towards fainter fluxes. The majority of the objects have indices $\Gamma \leq 1.7$. This flattening has been previously reported by Ueda et al. (1999) and Della Ceca et al. (1999). However, unlike the above, our sample consists exclusively of QSOs. Therefore it appears that over the hard band the QSOs show evidence for spectral hardening towards fainter fluxes.

The spectral analysis of the stacked spectrum shows that the *ASCA* yields an effective spectral index of $\Gamma = 1.56 \pm 0.18$, for type-1 QSOs. This is lower than the canonical spectral index of bright, nearby QSOs (eg Reeves et al. 1997, Lawson et al. 1998). In contrast, the above spectral

index is more consistent with the XRB spectrum (Gendreau 1995). Page (1997) studied the stacked spectrum of 34 *soft X-ray selected* QSOs from the RIXOS *ROSAT* survey using *ASCA*. He finds a spectral index of $\Gamma = 1.8 \pm 0.1$ consistent with that of QSOs in the 2-10 keV band. At first glance, the spectral flattening of the hard X-ray selected QSOs witnessed here could be due to intrinsic absorption. Indeed, a few high redshift QSOs with large amounts of absorption have been found so far in hard X-ray surveys (eg Fiore et al. 1999). However, in our case the *ROSAT* data do not favour this possibility.

The stacked *ROSAT* spectrum alone has a spectral index $\Gamma \approx 2.3$ consistent with the spectral index of individual soft X-ray selected QSOs in the soft 0.1-2 keV band (eg Laor et al., 1997, Fiore et al. 1998). Consequently, when we fit simultaneously the *ROSAT* and *ASCA* spectra, the data suggest the presence of a spectral upturn at soft energies. This upturn can be naively modeled with a black body component with $kT \sim 0.1$ keV, although this obviously has no physical interpretation. Then the power-law index becomes $\Gamma = 1.7 \pm 0.2$, in good agreement with the spectrum of nearby QSOs. Here, we note that Iwasawa, Nandra & Fabian (1999) raised some questions about the consistency of the *ROSAT* and *ASCA* spectral fits. In particular they fitted simultaneous *ROSAT* and *ASCA* spectra of NGC5548 finding that the *ROSAT* spectrum can be steeper by as much as $\Delta\Gamma \sim 0.4$ in the common 0.5-2 keV band. This discrepancy could be possibly attributed to uncertainties in the calibration of both *ROSAT* and *ASCA* instruments. Another possibility is that the concave spectrum obtained is an artefact of our assumption that the spectra of QSOs can be represented by a single value of Γ . More specifically the co-addition of spectra with steep and flat spectral indices may result in a steep and flat spectrum at low and high energies respectively. A final possibility is that the QSO spectra are indeed concave as

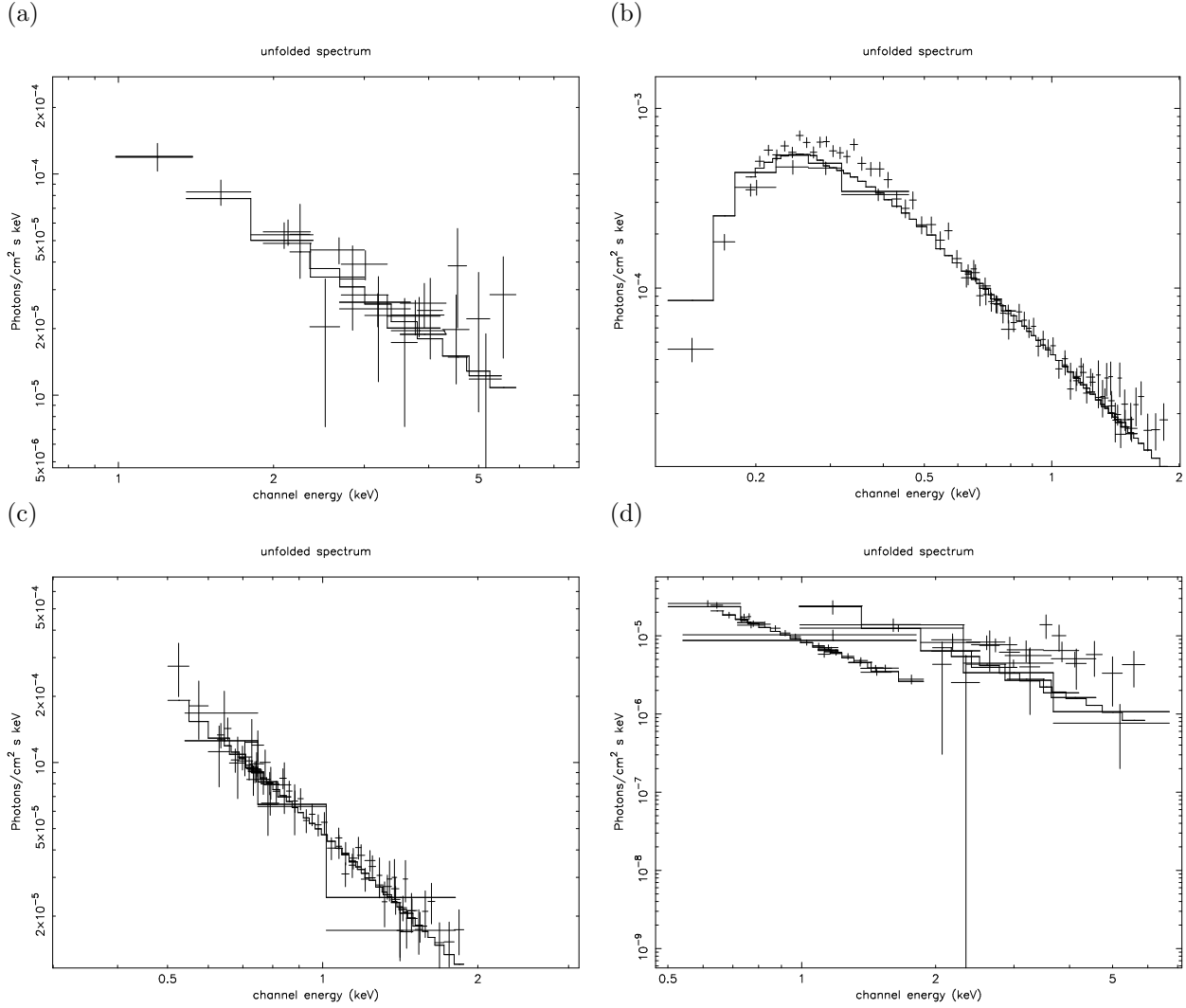


Figure 4. The unfolded spectrum for the power-law model for (a) the *ASCA* data over the 0.8–8.0 keV; (b) the *ROSAT* data over the 0.1–2.0 keV; (c) *ROSAT* data over the 0.5–2.0 keV and (d) the joint data over the 0.5–8.0 keV. The model fits are shown by solid histogram.

Table 3. Results of spectral fits, fixing the photoelectric absorption to the galactic values shown in Table 1.

	<i>ASCA</i> PL	<i>ROSAT</i> <i>PL</i> ^a	<i>ROSAT</i> <i>PL</i> ^b	<i>ASCA</i> - <i>ROSAT</i> PL	<i>ASCA</i> - <i>ROSAT</i> PL+BB	<i>ASCA</i> - <i>ROSAT</i> BKN PL
Γ	1.56 ± 0.18	2.32 ± 0.22	$2.44^{+0.01}_{-0.02}$	2.16 ± 0.1	$1.71^{+0.19}_{-0.17}$	2.35 ± 0.11
kT or E(keV)	-	-	-	-	0.1	$1.48^{+0.32}_{-0.19}$
Γ_2	-	-	-	-	-	$1.47^{+0.22}_{-0.20}$
$\chi^2(dof)$	104.89(99)	170.23(173)	690.69(333)	309.21(273)	271.46(261)	276(271)

^aspectral fitting in the 0.5–2.0 keV band

^bspectral fitting in the 0.1–2.0 keV band

originally suggested by Schwartz & Tucker 1988 (see also Mineo et al. 2000).

However, it is puzzling that in contrast with our results as well as the other *ASCA* and *BeppoSAX* results, *Chandra* has not found a large number of broad line QSOs with flat X-ray spectrum. In their hard selected sample only 2 QSOs were found. These have a spectral index Γ of ~ 1.8 . (Mushotzky et al. 2000). Possibly this is due to the sensitiv-

ity curve of *Chandra* which peaks below 2 keV and is lower than the *ASCA* sensitivity above ~ 7 keV and, therefore, possibly biases the results in favour of steep spectrum X-ray sources in the manner suggested by Della Ceca et al. (1999).

XMM-NEWTON with its high effective area as well its broad bandpass (0.1–12 keV) is expected to shed more light on the spectrum of individual, faint, high redshift QSOs which produce the largest fraction of the XRB.

6 ACKNOWLEDGMENTS

This research has made use of data obtained from the Leicester Database and Archive Service at the Department of Physics and Astronomy, Leicester University, UK.

REFERENCES

Akiyama M., et al. , 2000, ApJ, 532, 700
 Almaini O., Shanks T., Boyle B.J., Griffiths R.E., Roche N., Stewart G.C., Georgantopoulos I., 1996, MNRAS, 282, 295
 Antonucci R., 1993, ARA&, 31, 473
 Barger A. J., Cowie L. L., Sanders D. B., Fulton E., Taniguchi Y., Sato Y., Kawara K., Okuda H., 1998, Nat, 394, 248
 Blair A.J., Stewart G.C., Georgantopoulos I., Boyle B.J., Griffiths R.E., Shanks T., Almaini O., 2000, MNRAS, 314, 138
 Boyle, B.J., Staveley-Smith L., Stewart G. C., Georgantopoulos I., Shanks T., Griffiths R. E., 1993, MNRAS, 265, 501
 Boyle B.J., Staveley-Smith L., Shanks T., Georgantopoulos I., Stewart G.C., Griffiths R. E., 1995, Obs, 115,10
 Boyle B.J., Almaini O., Georgantopoulos I., Blair A.J., Stewart G.C., Griffiths R.E., Shanks T., Gunn K.F., 1998a, MNRAS, 297, 53L
 Boyle B.J, Georgantopoulos I., Blair A.J., Stewart G.C., Griffiths R.E., Shanks T., Gunn K.F., Almaini O., 1998b, MNRAS, 296, 1
 Boldt E., 1987, IAUS, 124, 611
 Cagnoni I., della Ceca R., Maccacaro T., 1998, ApJ, 493, 54
 Comastri A., Setti G., Zamorani G., Hasinger G., 1995, A&A,296, 1
 Condon J., Cotton W.D., Greisen E.W., Yin Q.F., Perley R.A., Taylor G.B., Broderick J.J., 1998, AJ, 115, 1639
 Della Ceca R., Castelli G., Braitto V., Cagnoni I., Maccacaro T.,1999, ApJ, 524, 674
 Di Matteo T., Allen S.W., 1999, ApJ, 527,L21
 Fabian A., 1999, MNRAS, 308, L39
 Iwasawa K., Fabian A.C., Nandra K., 1999, MNRAS, 307, 611
 Fiore F., Laor A., Elvis M., Nicastro F., Giallongo E., 1998, ApJ, 503, 607
 Fiore F. et al. 1999, MNRAS, 306, L55
 Fiore F., Comastra A., La Franca F., Vignali C., Matt G., Perola G. C., 2001, astro-ph/0102041
 Gendrau K.C., et al. , 1995, PASJ,, 47, L5
 Georgantopoulos I., Stewart G.C.,Shanks T., Boyle B.J., Griffiths R.E., 1996, MNRAS, 280, 276
 Georgantopoulos I., et al. , 1997, MNRAS, 291, 203
 Georgantopoulos I., Almaini O., Shanks T., Stewart G.C., Griffiths R.E., Boyle B.J., Gunn K.F., 1999, MNRAS, 305, 125
 Giacconi R., et al. , 1962, Phys. Review Letters, 9, 439
 Giacconi R., et al. , 2000, astro-ph/0007240
 Giommi P., Perri M., Fiore F., 2000, astro-ph/0006333
 Halpern J. P., Turner T. J., George I. M., 1999, MNRAS,307, L47
 Hughes D. H. et al., 1998, Nat, 394, 241
 Laor A., Fiore F., Elvis M., Wilkes B. J., McDowell J.C., 1997, ApJ, 477, 93
 Lawson A.J., Turner M.J.L., 1998, MNRAS, 288, 920
 Maiolino R. et al. , 2000, astro-ph/0002447
 Marshall F.,Boldt E.A., Holt S.S., Miller R.B., Mushotzky R.F., Rose L.A., Rothschild R.E., Serlemitsos P.J., 1980, ApJ, 235, 4
 Matt M.J., 1998, MNRAS, 298, 537
 Mineo et al. 2000, A&A, 361, 695
 Miyaji T., Hasinger G., Schmidt M., 2000, A&A, 353, 25
 Mushotzky R. F., Cowie L. L., Barger A. J., Arnaud K. A., 2000, Nature, 404, 459
 Nandra K., Pounds K.A., 1994, MNRAS, 268, 405
 Norman C., et al. 2001, astro-ph/0103198

Ohta K., Yamada T., Nakanishi K., Ogasaka Y., Kii T., Hayashida K., 1996, ApJ, 458, 57
 Parmar A.N., Guainazzi M., Oosterbroek T., Orr A., Favata F.,Lumb D., 1999, astro-ph/9903109
 Reeves J.N, 1999, PhD thesis, University of Leicester
 Reeves J.N, Turner M., 2000, MNRAS, 316, 234
 Schartel N., et al. , 1996, MNRAS, 283,101
 Schmidt M., et al. , 1998, A&A, 329, 495
 Setti G., Woltjer L., A&A, 224, 21L
 Schwartz D. A. & Tucker W. H., 1988, ApJ, 332, 157
 Stark A.A, Gammie C. F., Wilson R. W., Bally J. Linke R. A., Heiles C., Hurwitz M., 1992, ApJS, 79, 77
 Tanaka Y., Inoue H., Holt S.S., PASJ, 46, 37L
 Ueda Y., Takahashi Y., Ohashi T., Makishima K., 1999, ApJ, 524, 11
 Vecchi A., Molendi S., Guainazzi M., Fiore F., Parmar A.N., 1999, A&A, 349, 73
 Vignali C., Comastri A., Cappi M., Palumbo G.G.C., Matsuoka M., Kubo H., ApJ, 516, 582
 Vignali C., Mignoli M., Comastri A., Maiolino R., Fiore F., 2000, astro-ph/0002279
 Vikhlinin A., Forman W., Jones C., Murray S., 1995, ApJ, 451, 564